Downloaded from orbit.dtu.dk on: May 02, 2024

DTU Library

How to measure forces with atomic force microscopy without significant influence from nonlinear optical lever sensitivity

Thormann, Esben; Pettersson, Torbjön; Claesson, Per M.

Published in:
Review of Scientific Instruments

Link to article, DOI:
10.1063/1.3194048

Publication date:
2009

Document Version
Publisher's PDF, also known as Version of record

Link back to DTU Orbit

Citation (APA):
Thormann, E., Pettersson, T., & Claesson, P. M. (2009). How to measure forces with atomic force microscopy without significant influence from nonlinear optical lever sensitivity. *Review of Scientific Instruments*, *80*(9), Article 093701. https://doi.org/10.1063/1.3194048

General rights
Copyright and moral rights for the publications made accessible in the public portal are retained by the authors and/or other copyright owners and it is a condition of accessing publications that users recognise and abide by the legal requirements associated with these rights.

- Users may download and print one copy of any publication from the public portal for the purpose of private study or research.
- You may not further distribute the material or use it for any profit-making activity or commercial gain
- You may freely distribute the URL identifying the publication in the public portal

If you believe that this document breaches copyright please contact us providing details, and we will remove access to the work immediately and investigate your claim.

AIP | Review of Scientific Instruments

How to measure forces with atomic force microscopy without significant influence from nonlinear optical lever sensitivity

Esben Thormann, Torbjön Pettersson, and Per M. Claesson

Citation: Rev. Sci. Instrum. **80**, 093701 (2009); doi: 10.1063/1.3194048
View online: http://dx.doi.org/10.1063/1.3194048
View Table of Contents: http://rsi.aip.org/resource/1/RSINAK/v80/i9
Published by the AIP Publishing LLC.

Additional information on Rev. Sci. Instrum.

Journal Homepage: http://rsi.aip.org
Journal Information: http://rsi.aip.org/about/about_the_journal
Top downloads: http://rsi.aip.org/features/most_downloaded
Information for Authors: http://rsi.aip.org/authors

ADVERTISEMENT

Downloaded 11 Jul 2013 to 192.38.67.112. This article is copyrighted as indicated in the abstract. Reuse of AIP content is subject to the terms at: http://rsi.aip.org/about/rights_and_permissions

How to measure forces with atomic force microscopy without significant influence from nonlinear optical lever sensitivity

Esben Thormann,[a] Torbjön Pettersson, and Per M. Claesson
Department of Chemistry, Surface and Corrosion Science, Royal Institute of Technology, Drottning Kristinas Väg 51, SE-100 44 Stockholm, Sweden

(Received 26 February 2009; accepted 13 July 2009; published online 3 September 2009)

In an atomic force microscope (AFM), the force is normally sensed by measuring the deflection of a cantilever by an optical lever technique. Experimental results show a nonlinear relationship between the detected signal and the actual deflection of the cantilever, which is widely ignored in literature. In this study we have designed experiments to investigate different possible reasons for this nonlinearity and compared the experimental findings with calculations. It is commonly assumed that this nonlinearity only causes problems for extremely large cantilever deflections. However, our results show that the nonlinear detector response might influence many AFM studies where soft or short cantilevers are used. Based on our analysis we draw conclusions of the main reason for the nonlinearity and suggest a rule of thumb for which cantilevers one should use under different experimental conditions. © *2009 American Institute of Physics.* [doi:10.1063/1.3194048]

I. INTRODUCTION

During the past 2 decades the atomic force microscope (AFM) has proven to be an important tool for measuring surface and molecular forces. Interactions in the range from a few piconewtons to several micronewtons can be detected from the deflection of a micrometer-sized cantilever while the relative probe-surface separation is controlled by piezoelectric elements. By using the so-called colloidal probe technique,[1] AFM has been employed for direct measurements of surface forces.[2–9] In other cases AFM has been employed as an advanced tool for studies of biomolecular interactions on a single molecular scale,[10–14] or to studies of single polymer and protein mechanics.[15–20] Thus, AFM has become a widely used tool which compliments a range of other force sensing techniques such as the surface force apparatus, Optical tweezers, biomembrane force probe, etc.

Most commercial AFMs do, in principle, contain the basic elements shown in Fig. 1. The cantilever equipped with a probe (a micrometer-sized particle or a sharp tip) at the end, is the central part of the instrument. Interactions between the probe and a sample will lead to a vertical deflection and possible also to a lateral deflection of the cantilever, where the vertical and lateral deflections to a good approximation is proportional to the vertical and lateral component of the force between the probe and the surface (Hook's law). Vertical and lateral deflections of the cantilever are measured by reflecting a laser beam focused on the top side of the cantilever into a position sensitive detector. The relative motion of cantilever and sample is controlled by piezoelectric elements and feedback electronics with a precision in the order of 1 Å.[2]

To perform force-distance measurement the probe is normally first approached until (hard-wall) contact is reached and then subsequently retracted to the starting separation. During that process the change in the signal from the position sensitive detector as a function of the piezoextension is recorded. To transform this information into a force-distance relationship one needs to know the spring constant of the cantilever as well as a conversion factor between the detector signal and the cantilever deflection. Finding a reliable method for determination of the spring constant has been the subject of a large number of studies and several methods have been suggested.[21–27] However, assuring an accurate value of the conversion factor has normally been treated as a trivial issue, which has only been discussed in a few cases.[5,28–30] When the probe is in hard-wall contact with the surface it is assumed that further piezoextension translates into vertical cantilever deflection. Thus, from the slope of a straight line fitted to the signal in the hard-wall contact region one have a relationship between the vertical detector output, $\delta_V[V]$, and the true vertical cantilever deflection, $\delta_V[m]$. The inverse value of the slope, invOLS (inverse optical lever sensitivity), can thus together with the spring constant be used to calculate the force as

$$F = k \cdot \delta_V[m] = k \cdot \delta_V[V] \cdot \text{invOLS}. \quad (1)$$

From the description above, determining invOLS sounds as a trivial issue. However, the detector output is not completely linear even when measuring the interaction with a noncompliant surface. Thus, in principle no constant invOLS exists. This is illustrated in Fig. 2(a) where detector signal versus piezoextension for the approach and retraction motion are plotted. In Fig. 2(b), the hard-wall region has been emphasized together with the invOLS. The invOLS was determined by fitting a straight line to small different parts of the hard-wall contact region and from this plot it is clear that the invOLS is never constant but only has an almost constant value in a narrow region around in the beginning of the

[a]Author to whom correspondence should be addressed. Electronic mail: esben.thormann@surfchem.kth.se. FAX: +46 8208998.

Downloaded 11 Jul 2013 to 192.38.67.112. This article is copyrighted as indicated in the abstract. Reuse of AIP content is subject to the terms at: http://rsi.aip.org/about/rights_and_permissions

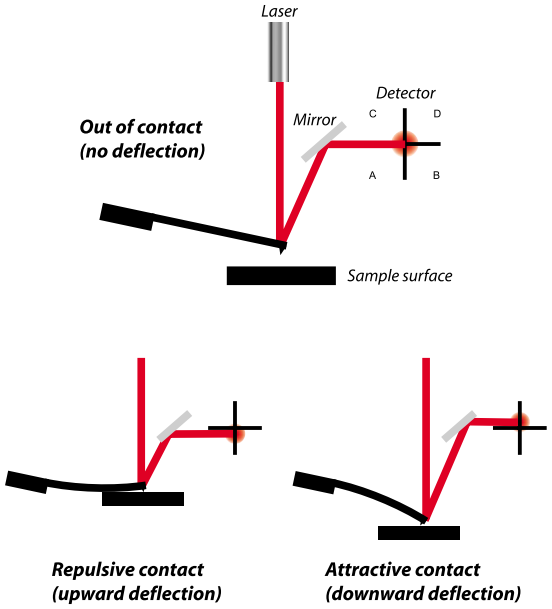

FIG. 1. (Color online) Top: Schematic illustration of the AFM setup. A laser beam is reflected at the back side of the cantilever and directed into a four-quadrant–split photodiode which is used to detect cantilever deflection. Bottom: Illustration of how repulsive contact (upward deflection) and attractive contact (downward deflection) moves the laser spot toward the two lower detector segments or the two upper detector segments, respectively.

hard-wall contact close to zero deflection. Nevertheless, the nonlinearity of the detector output in the contact region is widely ignored without further justification. In the following we investigate the reason for this nonlinearity and evaluate the consequences for force-distance experiments.

A. Background and hypotheses for nonlinearity

The position sensitive detector normally consists of a four-quadrant-split photodiode as shown in Fig. 1. When the laser spot hits the detector, a voltage proportional to the intensity of the light hitting each of the four segments are generated. We will refer to each of these voltage output as the V_A, V_B, V_C, and V_D signals, respectively. As illustrated in Fig. 1, an upward deflection of the cantilever originates from pressing the probe toward the surface (or from any other repulsive interaction), which results in that a fraction of the laser spot is transferred from the upper detector segments $(C+D)$ to the lower segments $(A+B)$. Similarly, a downward deflection originating from adhesion between the probe and the surface (or from any other attractive interaction) results in that a fraction of the laser spot is transferred from the two lower detector segments $(A+B)$ to the two upper segment $(C+D)$. In a similar manner, a lateral deflection of the cantilever will lead to a change in the fraction of the laser spot hitting the two left $(A+C)$ and the two right $(B+D)$ detector segments. Thus, the analog V_A, V_B, V_C, and V_D signal are inside the AFM used to determine the vertical and lateral deflection signals (measured in volts) as

$$\delta_V[V] = \frac{(V_A + V_B) - (V_C + V_D)}{V_A + V_B + V_C + V_D} \tag{2}$$

and

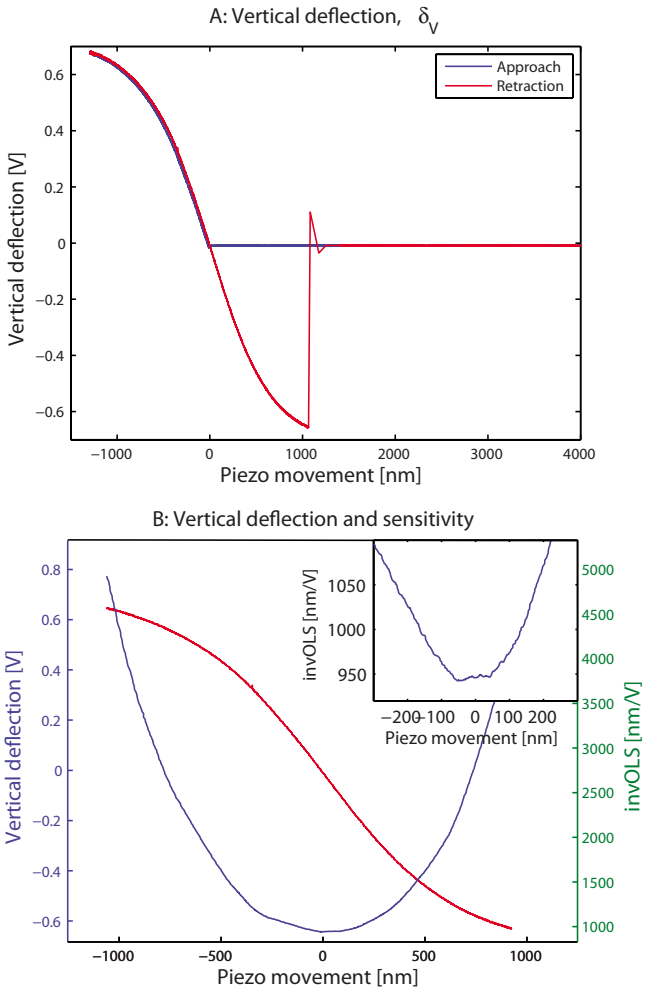

FIG. 2. (Color online) (a) Typical example of deflection vs piezomovement data for interaction between an AFM colloidal probe and a noncompliant mica surface in air. The data show a characteristic nonlinearity in the contact region. (b) The same data in the hard contact region and the invOLS for the same data range. The inset illustrates that the invOLS only has a nearly constant value in a narrow range around zero deflection.

$$\delta_L[V] = \frac{(V_A + V_C) - (V_B + V_D)}{V_A + V_B + V_C + V_D}. \tag{3}$$

These analog signals are subsequently amplified, digitalized, and sent to a computer. The digitalized deflection signals are together with the z-position the raw data available for the typical AFM-user and it is the $\delta_V[V]$ signal which shows the significant nonlinearity illustrated in Fig. 2(a). One can hypothesize different sources to the nonlinear response. Below we have listed eight possible contributions and denote these H1–H8.

H1: *Nonlinear relationship between cantilever deflection and laser spot movement.* It is, in general, assumed that there is a linear relationship between deflection of the cantilever and the laser spot movement on the position sensitive detector. However, this is based on some trigometric assumptions — e.g., that the angular deflection is small.

H2: *Laser light spilled over the cantilever edge.* At large downward deflections one could speculate that part of the laser light is spilled over the cantilever edge. This

Downloaded 11 Jul 2013 to 192.38.67.112. This article is copyrighted as indicated in the abstract. Reuse of AIP content is subject to the terms at: http://rsi.aip.org/about/rights_and_permissions

will result in a continuous decrease in the total laser intensity reaching the detector as the cantilever deflects.
H3: *Slipping.* If the probe is slipping on the surface it will have the consequence that not all piezomovement will translate into a vertical deflection.
H4: *Angle dependent reflection from the cantilever.* As the cantilever is deflecting the intensity of the laser beam reflected from the back side of the cantilever may be changing. The intensity of the deflected light depends on the angle of the cantilever relative to the incoming beam and on the material of the cantilever (or coating) and can be described by the so-called bidirectional reflectance distribution function.
H5: *Laser spot shape effect.* Since the position of the laser spot is detected by a split photodiode the intensity profile of the laser will limit how precisely the movement of the laser spot can be detected.
H6: *Laser light spilled over detector edge.* At large upward or downward deflections part of the laser spot might move outside the active part of the detector frame. This will result in both a change in the total laser intensity and in that the amount of light leaving one detector segment will not correspond to the amount of light entering another segment.
H7: *Unequal sensitivity of detector segments.* To obtain a linear detector response it is decisive that all parts of each detector segment have an equal sensitivity.
H8: *Photodetector saturation.* If the voltage output generated in a detector segment is not linear with respect to the intensity of laser light, it will lead to a nonlinear detector response at large cantilever deflections.

In the following we will investigate which of these possible contributions that are the important ones.

II. EXPERIMENTAL SECTION

Data presented in Sec. III originates from measurements between a spherical silica particle mounted on an AFM-cantilever and a freshly cleaved mica sheet. These measurements were performed in air at room temperature by use of a Nanoscope Multimode IIIa Pico Force atomic force microscope (Veeco Instruments). The silica particle ($d=6.9$ μm) was attached to a tipless cantilever (CSC 12F, MikroMasch) with no back side coating using a high-temperature melting epoxy glue (Epikote 1004, Shell Chemicals). Before attachment of the silica particle the spring constant of the cantilever was determined to 0.062 N/m by the Sader method.[25] All measurements were obtained at a constant approach and retraction velocity of 400 nm/s. A few data set presented in Sec. IV, represent measurements, performed in 0.01 mM NaCl aqueous solution, between a 20 μm silica particle and a mica surface. Silica particles of the same size were attached to three different cantilevers (CSC12E, CSC12F, and NSC12F, MikroMasch) as described above.

To access the raw voltage output from each of the four detector segments in the four-split photodiode a homemade breakout box was employed to split the signal. This means that part of the signal was sent to the AFM hardware as usual and another part of the signal was sent to a separate computer where the V_A, V_B, V_C, and V_D signals were captured simultaneously, followed by the z-position of the piezo, by means of two high-speed analog-to-digital converter data capturing cards (NI PCI-6132 and NI PCI-MIO-16E linked with a RTSI cable, National Instruments) and an in-house built Laboratory View (National Instrument) software. These data differs slightly from the data delivered to the computer through the AFM controller. Within the AFM, the voltage signals are amplified, digitalized, and processed in a way so that only the final vertical and lateral defection signals are available for the AFM user. During the digitalization process a certain deflection limit are used to set the bit resolution (we have used the maximum limit of ± 10 V). This means that the data are cut when the deflection signal exceeds that limit. In our setup the breakout box is located before the signals are amplified and further the deflection limit was set to cover the full range of the signal. However, after scaling the data with the amplification factor, the deflection calculated by Eq. (2) superimpose with the deflection signal processed by the AFM (within the predefined deflection limit).

III. RESULTS

A. Data output for optimal detector position

In the first experiment the laser spot was centered in the middle of the detector, which is the optimal and normal experimental configuration. During approach and retraction the intensity in each of the four photo detector segments as a function of the z-position were captured as described in Sec. II. Approach and retraction deflection curves superimposed in the repulsive part of the contact region as shown in Fig. 2(a), while during retraction the probe stayed in contact with the surface also in the attractive region due to strong adhesion. Thus the retraction curves provide us with a larger contact region that can be used to study the nonlinearity in the response. For simplicity we will therefore during the rest of this paper only focus on the contact region of the retraction curves. In Fig. 3 the outcome of the experiment is shown. The V_A, V_B, V_C, and V_D signals [Fig. 3(a)] are the direct output data while the sum signal, $V_A+V_B+V_C+V_D$ [Fig. 3(b)], the vertical deflection signal, δ_V [Fig. 3(c)], and the lateral deflection signal, δ_L [Fig. 3(d)] all are calculated from the V_A, V_B, V_C, and V_D signals. It should be mention that the V_A, V_B, V_C, and V_D signals have a constant offset of approximately -0.3 V which is the reason why the normalized deflection signal is going between -0.68 and $+0.68$ and not between -1 and 1. The V_A, V_B, V_C, and V_D signals show strong nonlinearity in an almost symmetric manner around the level of the signal in the noncontact region (zero deflection). This observation already gives us some information about the reason for the nonlinearity in the deflection signal shown in Fig. 2(a). For example, when the retraction starts, the cantilever has an upward deflection (hard-wall repulsion) that will decrease until zero deflection is reached. Hereafter downward deflection (adhesion contact) occurs. During this process light is transferred from the two lower segments ($A+B$) to the two upper segments ($C+D$) (see Fig. 1). Hence, if the nonlinearity only is an effect of photodetector saturation (H8) or due to that part of the laser lights is spilled over the

Downloaded 11 Jul 2013 to 192.38.67.112. This article is copyrighted as indicated in the abstract. Reuse of AIP content is subject to the terms at: http://rsi.aip.org/about/rights_and_permissions

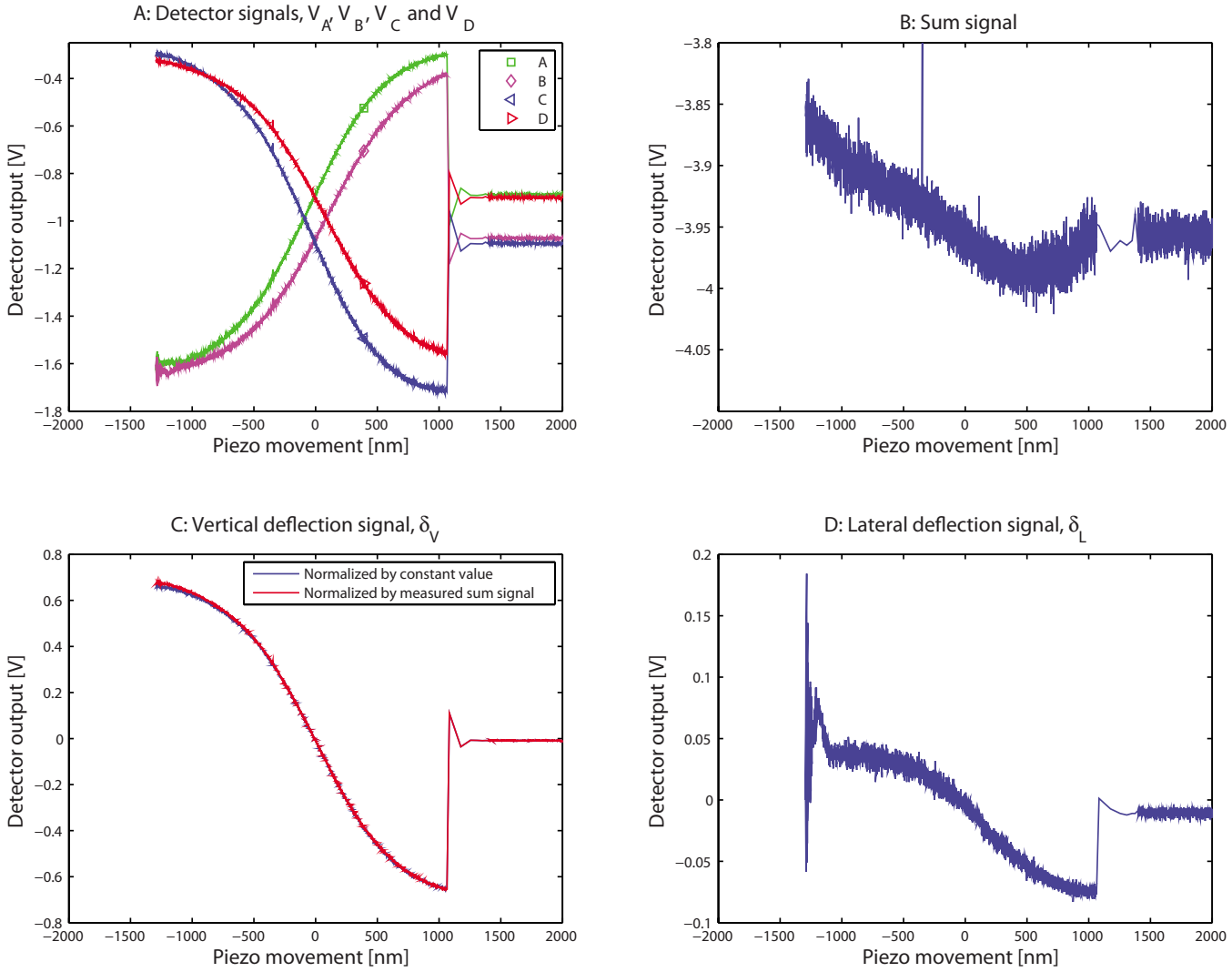

FIG. 3. (Color online) Data from experiment with the laser spot positioned centrosymmetric on the detector. Raw data output from the *A*, *B*, *C*, and *D* detector segments, respectively (a). Sum signal (b), vertical deflection (c), and lateral deflection (d) are all calculated from the *A*, *B*, *C*, and *D* signals.

detector edge (H6), each of the signals should be nonlinear in only one end of the contact region. The observation that all four signals are nonlinear at both ends of the contact region allows us to reject hypothesis H6 and H8, and suggests that other effects play a significant role.

From the sum signal in Fig. 3(b), one sees, as expected, that the sum signal has a constant value (within a low noise level) as long as the probe not is in contact with the surface. However, at both large upward and downward deflections the value is different from the constant value found out of contact. This could be due to photodetector saturation (H8), detector spill over (H6), or angle dependent scattering (H4). However, since both H6 and H8 already has been rejected based on the data in Fig. 3(a), we conclude that H4 must be the reason for this observation.

Figure 3(c) shows plots of the vertical deflection signal normalized by the sum signal [as given by Eq. (2)] and the deflection signal taken directly from the detector signals (normalized by the constant out-of-contact value of the sum signal). As already mentioned, the "raw" deflection signal from our AFM hardware is normalized by the sum signal. This is done to make it easy to compare forces/deflections independently of the magnitude of the sum signal. However, the basic assumption to justify this normalization is that the sum signal is constant during the approach-retraction cycle. As seen in Fig. 3(b) this condition is not fulfilled and the consequence is seen by the (small) difference between the two deflection plots at the highest degree of deflection in Fig. 3(c). The largest deviation is observed when the deflection signal already is highly nonlinear, and the error introduced by this assumption is thus not very significant in this case. However, as will be shown later, the assumption of a constant sum signal will be less valid in other cases. Therefore, in the following we will use the deflection signal normalized with a constant value (average of values measured when the tip is out of contact with the surface) to be able to compare this effect with other effects that are leading to the nonlinear deflection signal. Finally, the data in Fig. 3(d) show that the lateral deflection signal also changes in the contact region. The reason can be that the surface was slightly tilted. However, the magnitude of the lateral deflection is small compared to the normal deflection and the twisting motion is thus not the source of the significant nonlinearity in the vertical deflection signal. Further, the lateral deflection seems to

Downloaded 11 Jul 2013 to 192.38.67.112. This article is copyrighted as indicated in the abstract. Reuse of AIP content is subject to the terms at: http://rsi.aip.org/about/rights_and_permissions

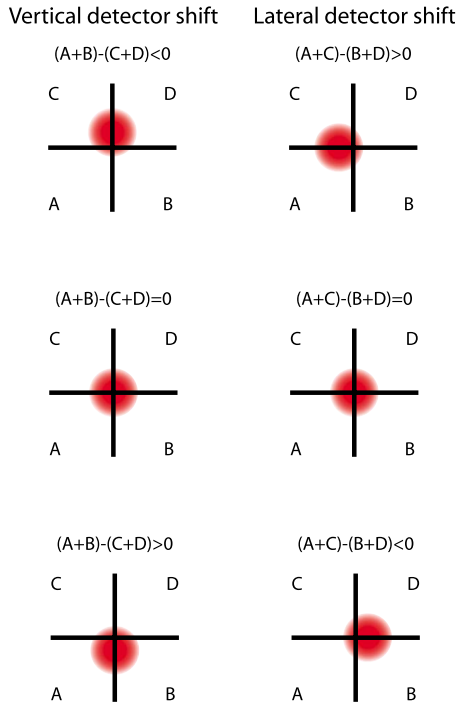

FIG. 4. (Color online) Normally the detector is positioned so that laser spot is at the center of the detector. However, in this study we have investigated how the detector signals are influenced by lateral and vertical shifts in the detector position as shown in the figure.

change most for small normal forces (small vertical deflection) while it reaches a plateau at high normal forces where the nonlinearity in the vertical deflection signal is most severe.

B. Data output with shifted detector position

In the following we have investigated how the signals discussed above are influenced by a shift in the laser spot position relative to the center of the detector (for a nondeflected cantilever). As illustrated in Fig. 4, the laser spot position was systematically shifted in vertical and lateral direction relative to the center of the detector. This was done by manually changing the detector position so that the amplified and the normalized lateral voltage difference were changed between −8 and +8 V in steps of 2 V, while keeping the vertical voltage difference constant at 0 V. Subsequently, the vertical voltage difference was shifted in a similar manner while the lateral voltage difference was kept constant at 0 V. As already mentioned above, we have collected the unamplified direct photodetector output. This means that in terms of the direct output the vertical and the lateral voltage difference was shifted in steps of an almost constant value of approximately 0.13 V. Figure 5 shows plots of the deflection signals, the sum signals and the V_A and V_C signals during a series of measurements with a lateral detector offset (the output from V_B and V_D are symmetric to those from V_A and V_C and are thus not shown).

The deflection signals shown in Fig. 5(a) have the same nonlinear behavior as observed in Fig. 3(c), and they do not change when the lateral voltage difference is changed between −8 and +8 V. All deflection curves nearly superimpose and the small change in the zero deflection value measured out of contact is due to small shifts in the vertical voltage difference that unavoidably occurred when the detector was laterally shifted. The data in Fig. 5(b) is similar to those in Fig. 3(b) and show that the sum signal is not constant in the contact region. Again, the results are independent of the shift in detector position. This means that no additional laser intensity is lost over the lateral edges of the detector (H6) when it is shifted left or right and in addition no sign of detector saturation (H8) or unequal segment sensitivity (H7) is observed during this experiment, which thus also allow us to reject hypothesis H7.

While no effect of changing the detector position laterally is seen on the deflection signals and the sum signals, an effect is naturally observed in the V_A and V_C signals [Figs. 5(c) and 5(d)]. Without further analysis three things are noticed from these plots. First, for extreme upward deflections the V_C signals, and for extreme downward deflections the V_A signals, go to a constant value of −0.3 V (independent of the lateral shift of the detector position) similar to what was observed in Fig. 3(a). This means that for these extreme deflections all light is hitting the two lower $(A+B)$ and two upper $(C+D)$ detector segments, respectively. Second, both the V_A and V_C signals increase as the lateral voltage difference is shifted toward more negative values as a larger fraction of the laser beam then reaches these two detector segments. Third, both the slope and range of the curves showing approximately linear response change with detector position. This latter point is a clear indication that the laser spot shape effect (H5) affects the measurements.

In Fig. 6, plots of the deflection signals, sum signals and the V_A and V_C signals from a series of measurements with a vertical detector offset are shown. Clearly, a vertical detector offset has an effect on the vertical deflection signal. The out of contact value is vertically shifted by the offset of 0.13 V which is expected. This also leads to that the whole deflection signal is shifted sideways. Also as expected, around the zero position of the piezomovement the deflection signals have the same values as the out of contact values for the same curves. The signals in the contact region show a number of interesting features. For extreme upward deflections (hard-wall repulsion) all deflection signals follow each other and go to a constant value of approximately 0.68 V. For extreme downward deflections (due to adhesion) the deflection signals reach different values before the particle detaches from the surface and jumps out of contact. One very important observation is that all contact curves have the same shape independently of the vertical detector offset. For example, the approximately linear parts of the deflection signals are always centered around 0V. This shows that the onset of the nonlinearity mainly is related to the position of the laser spot on the detector (H5) and is not directly due to how much the cantilever is deflected. A nonlinear relationship between cantilever deflection and laser spot movement (H1) or laser light spill over the cantilever edge during extreme downward deflection (H2) would result in different deflection signals around 0V, while slip between the probe and the surface (H3) would depend strongly on the actual deflection. Thus, we can reject hypothesis H1, H2, and H3.

Downloaded 11 Jul 2013 to 192.38.67.112. This article is copyrighted as indicated in the abstract. Reuse of AIP content is subject to the terms at: http://rsi.aip.org/about/rights_and_permissions

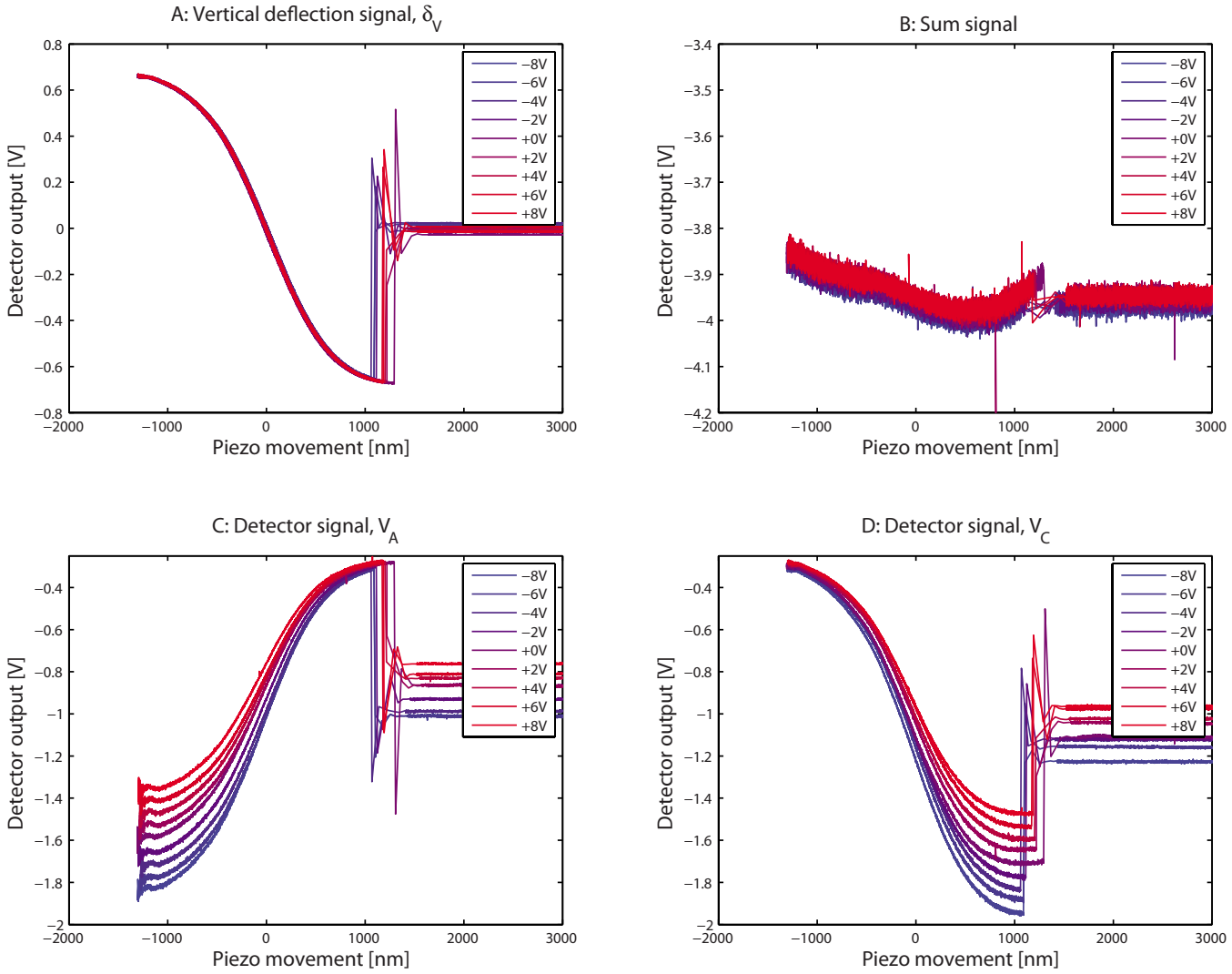

FIG. 5. (Color online) Detector outputs obtained with lateral offsets of the detector position. The amplified signal which is sent to the AFM hardware was changed in steps of 2 V between −8 to +8 V by manually moving the detector with respect to the laser beam.

For a large negative detector offset an interesting observation can be made at the most extreme downwards deflections. At a value of approximately −2.6 V there is a turning point where the numerical value of the deflection signal starts to decreases. However, since the probe still is in surface contact, the cantilever should be more deflected, and hence the numerical value of the deflection signal ought to increase. The interpretation of this phenomenon is as follows: When the cantilever starts to deflect downwards light is transferred from the two lower segments $(A+B)$ to the two upper segments $(C+D)$. However, after the turning point more light actually leaves the two upper segments than the lower segments. This is most likely an effect of the angle dependent scattering (H4), which is supported by the results shown in Fig. 6(b), that illustrates how the change in sum signal is affected by the vertical detector offset. The sum signals are not significantly affected by a shift in vertical detector position when the cantilever is deflected upwards. However, at large downwards deflections it is observed that the numerical value of the sum signal decreases rapidly for a large negative detector offset. This supports the conclusions drawn from the deflection signals in Fig. 6(a), namely, that the combination of a large detector offset and a large deflection leads to a loss in signal intensity. On the other hand, for vertical detector offsets between −4 and +8 V (on the AFM) the sum signal is unaffected by the shift in detector position. This is the same range of detector offset where no turning points were observed in the corresponding deflection curves.

In Figs. 6(c) and 6(d), the V_A and V_C signals are plotted. Again, it is observed that the signals superimpose and that the signal in the contact region only depends on the laser spot position and not on the actual cantilever deflection. From these plots the reason for the turning points observed in Fig. 6(a) becomes confirmed. For negative detector offsets and large downward deflections a similar turning point are observed in the V_C signal [Fig. 6(d)] and at the same time the V_A signal reaches a plateau at approximately −0.3 V [Fig. 6(c)]. At this point the hole laser spot has been transferred to the lower detector segments at the same time as the total laser intensity is decreasing due to hypothesis H4. Thus, the turning point in the V_C signal.

Combining all of our data leads to the conclusion that the nonlinearity mainly is due to a laser spot shape effect

Downloaded 11 Jul 2013 to 192.38.67.112. This article is copyrighted as indicated in the abstract. Reuse of AIP content is subject to the terms at: http://rsi.aip.org/about/rights_and_permissions

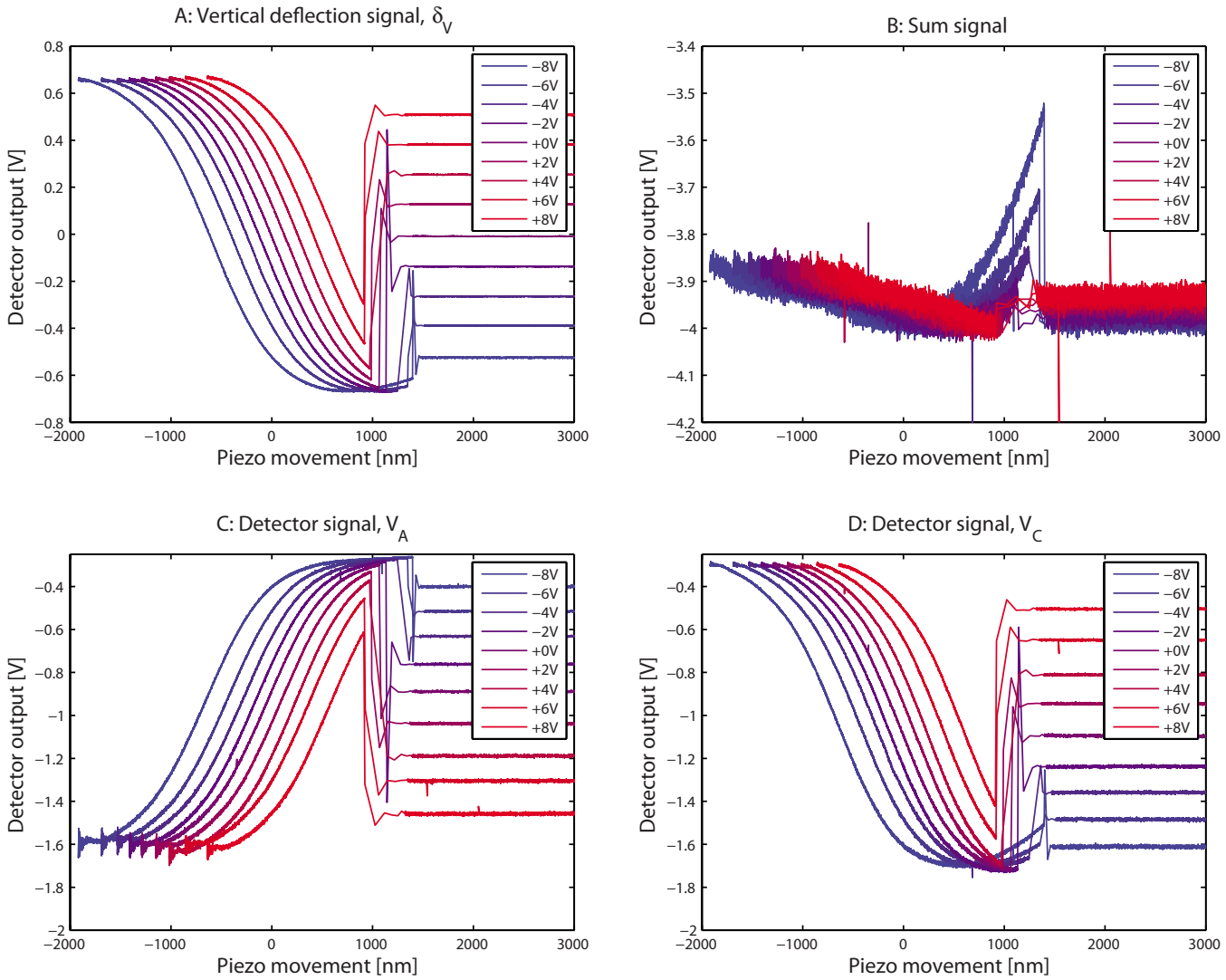

FIG. 6. (Color online) Detector outputs obtained with vertical offsets of the detector position. The amplified signal which is sent to the AFM hardware was changed in steps of 2 V between −8 to +8 V by manually moving the detector with respect to the laser beam.

(H5), angle dependent scattering from the cantilever (H4) or both.

IV. DISCUSSION

From the results above we have narrowed the possible reasons to the nonlinear detector response down to the effect of angle dependent scattering from the cantilever (H4) and the effect of the laser spot shape and intensity distribution (H5). Further, the nonlinear relationship between cantilever deflection and laser spot movement (H1) can also be addressed from a theoretical point of view.

A. Cantilever deflection versus laser spot movement

The results do not show any direct evidence for a nonlinear relationship between cantilever deflection and laser spot movement (H1). However, the issue can also be addressed theoretically. Figure 7(a) shows a sketch of how the path of the reflected laser light is changed due to deflection of the cantilever. As seen in this figure, the distance which the laser spot has moved on the detector is related to the degree of deflection as

$$\Delta S = 2(L + L')\tan(\alpha) \approx 2L\alpha \quad \text{for } L \gg L' \text{ and small values of } \alpha, \tag{4}$$

where ΔS is the change in position of the laser spot on the detector, L is the length between the point of reflection on the cantilever and the detector (approximately 6 cm for our system), α is the angle of the deflected cantilever at the laser beam position, and L' is a length defined in Fig. 7. We note that the optical lever technique is sensitive to the angle of the deflected cantilever (at the position of laser reflection) rather than to the deflection, δ_V. However, by considering the physics of bending a cantilever the slope can be related to the deflection. If an end-loaded force is applied to a cantilever with uniform material properties and if the laser spot is positioned at the very end of the cantilever, the relation is

$$\Delta S = \frac{3L}{l}\delta_V. \tag{5}$$

From these two expressions we obtain $\delta_V/l = 2/3\ \tan(\alpha)$, and there is a linear relationship between the cantilever deflection and the movement of the laser spot as long as $\delta_V/l \approx 2/3\alpha$. From Fig. 7(b) it is seen that this condition is fulfilled when

Downloaded 11 Jul 2013 to 192.38.67.112. This article is copyrighted as indicated in the abstract. Reuse of AIP content is subject to the terms at: http://rsi.aip.org/about/rights_and_permissions

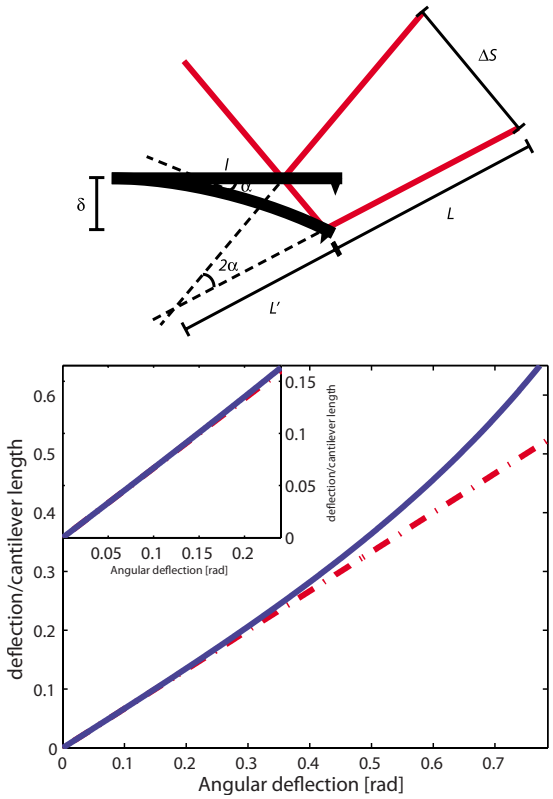

FIG. 7. (Color online) Top: Deflection of a cantilever measured with the optical lever technique. A cantilever with length l is deflected by a distance δ_V and an angle α. ΔS is the distance the laser spot has moved due to the deflection and L is the distance from the point of reflection to the detector. Bottom: Relationship between cantilever deflection and angular deflection—the relationship is approximately linear for $\delta/l \lesssim 0.1$.

$\delta_V/l \lesssim 0.1$. From Fig. 2 it is seen that for the results presented in this study the largest deflection is ≈ 1 μm, meaning that in this case with strong adhesion and a fairly soft cantilever, $\delta_V/l = 1$ μm/250 μm=0.004 which is far below the value where nonlinearity will occur. It should be emphasized that this will be true for all relevant experimental conditions since measuring stronger forces with even weaker cantilevers will be invalid for other reasons as will be discussed below. Thus, we can disregard hypothesis H1 also on theoretical grounds.

B. Correction for lost laser intensity

Our results have clearly demonstrated that the total intensity of the laser beam reaching the detector depends on the actual deflection of the cantilever as expected from the so-called bidirectional reflectance distribution function (which depends on the cantilever material or back side coating). Thus, when the cantilever starts to deflect and the laser spot thereby starts to move over the detector, the decrease in the amount of photons hitting one detector segment will not correspond to a similar increase in the amount of photons hitting another detector segment. We have also clearly demonstrated that this effect is one reason for the nonlinearity in the detector response observed in Figs. 3, 5, and 6. However, one can easily correct for this effect by normalizing the V_A, V_B, V_C, and V_D signals by the measured sum signal at any given time. This is actually what is done as default by the AFM hardware, and this is correct if the change in sum signal solely is an effect of the bidirectional reflectance distribution function. Since our data demonstrate that this is the case, we can thus, after the correct normalization, disregard hypothesis H4.

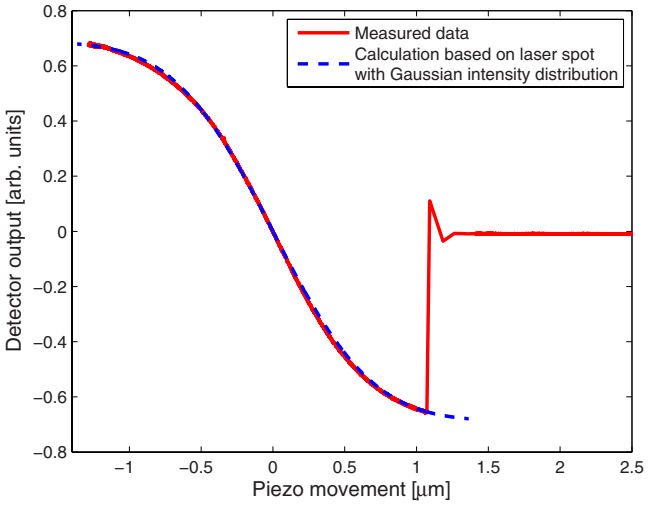

FIG. 8. (Color online) The full line is representing experimental data of the deflection signal which is showing strong nonlinearity in the contact region. Each of the A, B, C, and D detector outputs were added a constant offset value of +0.3 V and the deflection signal was subsequently calculated by Eq. (2). The dotted line is showing calculated values of how the deflection signal is expected to look like if one assume a laser spot with a Gaussian intensity distribution with a standard deviation, $\sigma = 120$ μm. As seen is the nonlinearity in the experimental data very well described by the laser spot shape effect.

C. The laser spot shape effect

We have now rejected all hypothesis, except from hypothesis H5, which will thus be analyzed further in this section.

Moving the laser spot a given fixed distance over the detector will lead to a transfer of light from the two lower detector segments to the two upper segments (or vice versa). However, since the intensity of the light decreases with the distance to the center of the spot, the amount of light transferred depends on the initial position of the laser spot on the detector. This means that the transfer rate is highest when the spot is centered in the middle of the detector while it decreases as the spot is moved away from this position.

If it is assumed that the laser spot has a spherical shape with a Gaussian intensity distribution, the total measured intensity of the light hitting the detector will be given as

$$I = \int \int \frac{A}{2\pi\sigma} \exp\left(-\frac{S_v^2 + S_l^2}{2\sigma^2}\right) dS_v dS_l, \tag{6}$$

where σ is the standard deviation defining the width of the intensity distribution, S_v and S_l are the vertical and lateral directions on the detector, and A is a scaling factor determining the total absolute intensity. The vertical deflection signal as defined by Eq. (2) is thus found by integration of Eq. (6) along the S_v-axis. By adjusting σ and correlating the laser spot movement to the cantilever deflection by Eq. (5), this calculated detector output can be directly compared to measure data.[31] This is done in Fig. 8 where it is seen that with a standard deviation, $\sigma = 120$ μm, an almost perfect

Downloaded 11 Jul 2013 to 192.38.67.112. This article is copyrighted as indicated in the abstract. Reuse of AIP content is subject to the terms at: http://rsi.aip.org/about/rights_and_permissions

agreement between the measured and the calculated detector output is found. This result strongly supports our experimental finding—the nonlinearity in the measured deflection signal is mainly due to the intensity distribution of the laser spot.

D. Choice of cantilever

The aim of this study was not solely to explore the reasons for the nonlinearity in the detector response, but also to evaluate how it possibly can affect experimental results. This study has clearly demonstrated that problems occur if the laser spot movement becomes too large. The problem can thus easily be minimized if one always chooses a cantilever with proper stiffness and dimensions compared to the magnitude of the maximum force one wants to measure. For a given cantilever length that means: soft cantilevers for measurement of weak forces and stiff cantilevers for measurements of strong forces. Based on the results presented in this paper one can estimate the maximum cantilever deflection one should reach in a given experiment and thus also the optimal relation between cantilever stiffness and cantilever length as

$$\delta_V > \frac{l}{3L}\Delta S^{\text{linear}} \tag{7}$$

and

$$kl > \frac{F_{\max}}{\delta_V^{\max}} = F_{\max}\frac{3L}{\Delta S^{\text{linear}}}, \tag{8}$$

where $F_{\max}$ is the maximum force that will be measured, $\delta_V^{\max}$ is the maximum cantilever deflection which still gives an approximately linear detector output, and ΔS^{linear} is the corresponding maximum movement of the laser spot on the detector (away from the detector center) which still gives an approximately linear detector output. From the results presented in Fig. 8 it is found that $\Delta S^{\text{linear}} \approx \frac{1}{2}\sigma$. Thus for our particular system it is found that

$$\delta_V > \frac{l\sigma}{6L} \approx \frac{(250\times10^{-6}\ \text{m})(120\times10^{-6}\ \text{m})}{6(6\times10^{-2}\ \text{m})} = 83\ \text{nm} \tag{9}$$

and

$$kl > F_{\max}\frac{6L}{\sigma} \approx F_{\max}\frac{6(6\times10^{-2}\ \text{m})}{120\times10^{-6}\ \text{m}} = 3000F_{\max}, \tag{10}$$

which means that the maximum force one should measure with the cantilever used here is ± 5 nN (or $F_{\max}/R = \pm 0.7$ mN/m). The length of the optical pathway, L, and standard deviation, σ, of the laser spot intensity distribution will of course vary slightly between different instruments. Thus, the exact numbers in Eq. (10) will not be generally valid and should be confirmed for each particular instrument. However, since L not is likely to vary significantly between different commercial AFMs we suggest that as a rule of thumb, $kl > 3000F_{\max}$, as a criteria which should be approximately valid in most situations. Since the lever rule given by Eq. (5) depends on the length but not on the geometry of the cantilever, this rule of thumb works for all cantilever geometries (e.g., rectangular or triangular).

It might sound obvious to use soft or stiff cantilevers depending on the magnitude of the forces to be measured. However, since soft and stiff is a qualitative description and since stiffer cantilevers often also gets shorter it is not easy to identify the right choice of cantilever without an estimate as shown above. The literature is full of examples of interesting AFM-based force-separation measurements where this issue has never been considered. Measuring adhesion forces with a too weak or short cantilever seems to be very common,[6,32–35] and it has the effect that the magnitude of the reported forces will be too small if the adhesion force is calculated from the cantilever deflection (and not from the jump-out distance, $F_{\text{adhesion}} = kD_{\text{jump-out}}$). In friction studies it is common to measure the friction force versus the applied normal load.[8,36–39] If a too weak or short cantilever is used in such cases it means that the true applied load will be higher than the apparent applied load. This will give rise to nonlinearity in plots of friction force versus applied load. For measurements of short- or long-range surface force, the use of a too weak or short cantilever[40–43] will not only lead to a too small magnitude of the measured forces but also to an error in the curve shape and thus to possible wrong conclusions about the underlying mechanism of the interaction. In most single molecule studies the cantilevers are properly chosen since the forces are generally very weak.[10–16] However, their are examples of single polymer stretching experiments where the measured force reaches large magnitudes.[19,44,45] In such a case an error in the curve shape is introduced, making comparisons with theoretical models problematic.

The effect of cantilever stiffness and length on the measured detector output is illustrated in Fig. 9. The electrostatic double layer force between a ≈ 20 μm-sized silica particle and a mica surface in 0.01 mM NaCl is here probed by three different cantilevers. The out-of-contact interaction measured by the softest cantilever ($k=0.023$ N/m, $l=350$ μm) leads to laser spot movement which is not within the approximately linear range of the detector. This is also the case for the interaction measured by the cantilever of intermediate stiffness ($k=0.064$ N/m, $l=250$ μm). The main reason for this is that this cantilever also is significantly shorter than the softest cantilever. Thus, although a stiffer cantilever leads to a smaller deflection for the same interaction, the shorter length of this cantilever leads to a relatively larger laser spot movement as in according with Eq. (5). Finally, both the out-of-contact and contact interaction measured by the stiffest cantilever ($k=0.54$ N/m, $l=250$ μm) shows to be well within the linear range of the detector. This cantilever is stiffer due to its larger thickness and not to a reduced length. This illustrate that, in agreement with the relation stated in Eq. (10), both cantilever stiffness and length are important quantities.

E. Concluding remarks

During the studies presented in this paper it was found that the observed nonlinearity in the detector output originating from the vertical deflection of the AFM cantilever in a

Downloaded 11 Jul 2013 to 192.38.67.112. This article is copyrighted as indicated in the abstract. Reuse of AIP content is subject to the terms at: http://rsi.aip.org/about/rights_and_permissions

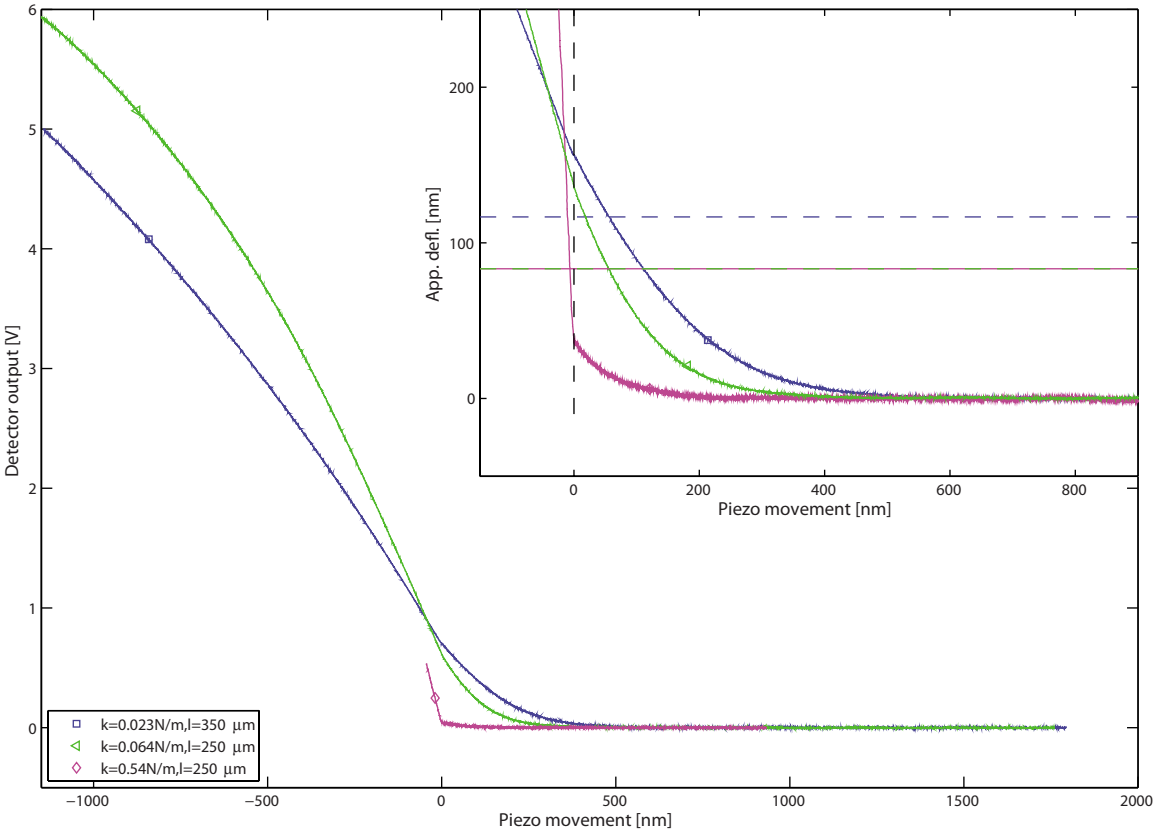

FIG. 9. (Color online) Detector outputs generated by interaction between a 20 μm-sized silica particle and a mica surface in 0.01 mM NaCl by use of three different cantilevers. The two softest cantilevers show clearly nonlinear detector response both in the out-of-contact and contact interaction region while the stiffest cantilever (which, to avoid surface damage, was not pressed to the same level of deflection) show a linear detector response in the full measured range. The inset shows the apparent deflection base on the apparent invOLS obtained from the hard-wall contact region. Here the deflection of the stiffest cantilever has been up scaled ten times for better visualization. Based on Eq. (9) the upper vertical line provide and maximum allowed deflection for the softest cantilever while the lower vertical line provide and maximum allowed deflection for the two stiffest cantilevers. Notice that this maximum value has not been up scaled and that the stiffest cantilever, which thus is deflected to a value that is approximately twenty times smaller than the maximum allowed value, is the only one which follows our rule of thumb for the relationship between cantilever stiffness, cantilever length and the maximum measured force.

force-separation measurement could be narrowed down to two contributions.

First, it was found that the total intensity of the light reflected from the cantilever and directed to the detector was dependent on the deflection of the cantilever. This will lead to a nonlinearity in the deflection signal only if it is not normalized by the sum signal, and since this normalization normally is done during the data processing in commercial instruments this effect is not a concern for the normal AFM user. However, for more nonstandardized experiments where detector signals are read directly from the detector (by use of a breakout box) it is important to be aware of this fact.

Second, it was found that the most important source for the nonlinearity is the shape and intensity distribution of the laser light hitting the detector. It was shown that the nonlinearity in experimentally obtained deflection curves could be predicted by assuming a spherical laser spot with a Gaussian intensity distribution.

This nonlinearity in the detector signal is of concern when determining the inverse optical lever sensitivity (invOLS), which is needed in order to convert detector output into real cantilever deflection. This study shows that the invOLS only has an approximative constant value for small laser spot movements when the laser spot initially has been positioned in the center of the detector. This implies that the invOLS only can be determined correctly when no additional surface forces (as long-range electrostatic or steric repulsion) adds significantly to the hard-wall repulsion. If additional surface forces are present, hard-wall repulsion will not be reach at the required small laser spot movements. Thus, to achieve the correct results the invOLS should, e.g., be determined by obtaining a force-distance curve between noncompliant surfaces in an aqueous solution of high ionic strength.

Finally, we have also shown that the nonlinearity sets a limitation for the magnitude of the force which can be measured correctly with a given cantilever. We find a trend that to weak and short cantilevers are used in many AFM studies and that this can cause both errors in the magnitude of the measured forces and in the shape of the force curves. Based on our analysis we suggest a rule of thumb for the relation between cantilever stiffness, cantilever length, and the magnitude of the maximum measured force: $kl > 3000F_{\max}$. We note that $F_{\max}$ is the absolute value of the maximum measured attractive or repulsive force or the maximum in the constant compliance region used for the data analysis. This rule of thumb also implies that one should choose a thicker cantilever rather that a shorter cantilever if one wants to increase the cantilever stiffness to get within the linear detector range.

Downloaded 11 Jul 2013 to 192.38.67.112. This article is copyrighted as indicated in the abstract. Reuse of AIP content is subject to the terms at: http://rsi.aip.org/about/rights_and_permissions

ACKNOWLEDGMENTS

E.T. gratefully acknowledge financial support from the European Community's Marie Curie Research Training Network "Self Organisation under Confinement (SOCON)," Contract No. MRTN-CT-2004-512331 and from the excellence center "Controlled Release and Delivery Centre (Codirect)." T.P. and P.M.C. acknowledge financial support from the Swedish Research Council (VR).

[1] W. A. Ducker, T. J. Senden, and R. M. Pashley, Nature (London) **353**, 239 (1991).
[2] B. Cappella and G. Dietler, Surf. Sci. Rep. **34**, 1 (1999).
[3] P. M. Claesson, T. Ederth, V. Bergeron, and R. W. Rutland, Adv. Colloid Interface Sci. **67**, 119 (1996).
[4] T. J. Senden, Curr. Opin. Colloid Interface Sci. **6**, 95 (2001).
[5] H.-J. Butt, B. Cappella, and M. Kappl, Surf. Sci. Rep. **59**, 1 (2005).
[6] E. Thormann, A. C. Simonsen, P. L. Hansen, and O. G. Mouritsen, Langmuir **24**, 7278 (2008).
[7] E. Thormann, A. C. Simonsen, P. L. Hansen, and O. G. Mouritsen, ACS Nano **2**, 1817 (2008).
[8] T. Pettersson and A. Dedinaite, Adv. Colloid Interface Sci. **324**, 246 (2008).
[9] T. Pettersson, Z. Feldötö, P. M. Claesson, and A. Dedinaite, Prog. Colloid Polym. Sci. **134**, 1 (2008).
[10] G. U. Lee, D. A. Kidwell, and R. J. Colton, Langmuir **10**, 354 (1994).
[11] T. Strunz, K. Oroszlan, R. Schäfer, and H.-J. Güntherodt, Proc. Natl. Acad. Sci. U.S.A. **96**, 11277 (1999).
[12] C.-K. Lee, Y.-M. Wang, L.-S. Huang, and S. Lin, Micron **38**, 446 (2007).
[13] E. Thormann, P. L. Hansen, A. C. Simonsen, and O. G. Mouritsen, Colloids Surf., B **53**, 149 (2006).
[14] E. Thormann, J. K. Dreyer, A. C. Simonsen, P. L. Hansen, S. Hansen, U. Holmskov, and O. G. Mouritsen, Biochemistry **46**, 12231 (2007).
[15] M. Rief, M. Gautel, F. Oesterhelt, J. M. Fernandez, and H. E. Gaub, Science **276**, 1109 (1997).
[16] F. Oesterhelt, M. Rief and H. E. Gaub, New. J. Phys. **1**, 6 (1999).
[17] M. Carrion-Vazquez, A. F. Oberhauser, S. B. Fowler, P. E. Marzalek, S. E. Broedel, J. Clarke, and J. M. Fernandez, Proc. Natl. Acad. Sci. U.S.A. **96**, 3694 (1999).
[18] H. Li, W. Zhang, W. Xu, and X. Zhang, Macromolecules **33**, 465 (2000).
[19] T. Hugel, M. Grosholz, H. Clausen-Schaumann, A. Pfau, H. Gaub, and S. Seitz, Macromolecules **34**, 1039 (2001).
[20] E. Thormann, D. R. Evans, and V. S. J. Craig, Macromolecules **39**, 6180 (2006).
[21] J. L. Hutter and J. Bechhoefer, Rev. Sci. Instrum. **64**, 1868 (1993).
[22] J. P. Cleveland, S. Manne, D. Bocek, and P. K. Hansma, Rev. Sci. Instrum. **64**, 403 (1993).
[23] T. J. Senden and W. A. Ducker, Langmuir **10**, 1003 (1994).
[24] C. T. Gibson, G. S. Watson, and S. Myhra, Nanotechnology **7**, 259 (1996).
[25] J. E. Sader, J. W. M. Chon, and P. Mulvaney, Rev. Sci. Instrum. **70**, 3967 (1999).
[26] N. A. Burnham, X. Chen, C. S. Hodges, G. A. Matei, E. J. Thoreson, C. J. Roberts, M. C. Davies, and S. J. B. Tendler, Nanotechnology **14**, 1 (2003).
[27] P. J. Cumpson, Ultramicroscopy **100**, 241 (2004).
[28] G. Haugstad and W. L. Gladfelter, Ultramicroscopy **54**, 31 (1994).
[29] P. Attard, T. Pettersson, and M. W. Rutland, Rev. Sci. Instrum. **77**, 116110 (2006).
[30] M. J. Higgins, R. Proksch, J. E. Sader, M. Polcik, S. Endoo, J. P. Cleveland, and S. P. Jarvis, Rev. Sci. Instrum. **77**, 013701 (2006).
[31] Before calculating the normal deflection from the measured data, a constant value of +0.3 V was added to each of the *A*, *B*, *C*, and *D* detector output to correct for the constant detector offset of −0.3 V. As discussed in the results section this is needed if one wants the normalized deflection signal to vary between −1 and 1.
[32] W. R. Bowen, N. Hilal, R. W. Lovitt, and C. J. Wright, Colloids Surf., A **157**, 117 (1999).
[33] J. W. Kurutz and S. Xu, Langmuir **17**, 7323 (2001).
[34] D. M. Jones, J. R. Smith, W. T. S. Huck, and C. Alexander, Adv. Mater. (Weinheim, Ger.) **14**, 1130 (2002).
[35] A. Sethuraman, M. Han, R. S. Kane, and G. Belfort, Langmuir **20**, 7779 (2004).
[36] J. Hu, X.-D. Xiao, D. F. Ogletree, and M. Salmeron, Surf. Sci. **327**, 358 (1995).
[37] A. Marti, G. Haehner, and N. D. Spencer, Langmuir **11**, 4632 (1995).
[38] V. N. Koinkar and B. Bhushana, J. Vac. Sci. Technol. A **14**, 2378 (1996).
[39] E. Taran, Y. Kanda, I. U. Vakarelski, and K. Higashitani, J. Colloid Interface Sci. **307**, 425 (2007).
[40] T. A. Camesano and B. E. Logan, Environ. Sci. Technol. **34**, 3354 (2000).
[41] P. G. Hartley, F. Grieser, P. Mulvaney, and G. W. Stevens, Langmuir **15**, 7282 (1999).
[42] S. Veeramasuneni, M. R. Yalamanchili, and J. D. Miller, J. Colloid Interface Sci. **184**, 594 (1996).
[43] S. Kidoaki, S. Ohya, Y. Nakayama, and T. Matsuda, Langmuir **17**, 2402 (2001).
[44] Y. Ying, W. Fang, S. WeiQing, W. LiYan, W. WenBin, and S. JiaCong, Chin. Sci. Bull. **53**, 22 (2008).
[45] M. A. K. Williams, A. Marshall, R. G. Haverkamp, and K. I. Draget, Food Hydrocolloids **2008**, 22 (2008).

Downloaded 11 Jul 2013 to 192.38.67.112. This article is copyrighted as indicated in the abstract. Reuse of AIP content is subject to the terms at: http://rsi.aip.org/about/rights_and_permissions